Sains Malaysiana 54(6)(2025): 1593-1604
http://doi.org/10.17576/jsm-2025-5406-14

Enhanced Solubility and Dissolution of Ketoconazole through Co-Amorphization with Fumaric and Tartaric Acids *via* Co-Milling

(Peningkatan Keterlarutan dan Pelarutan Ketokonazol melalui Amorfisasi Bersama dengan Asid Fumarik dan Asid Tartarik melalui Pengisaran Bersama)

INDRA INDRA[1,*], RANI NURANI[1] & WINDA TRISNA WULANDARI[2]

[1]*Pharmaceutics Group, Faculty of Pharmacy, Universitas Bakti Tunas Husada, Tasikmalaya, 46115, Indonesia*
[2]*Pharmacochemistry Group, Faculty of Pharmacy, Universitas Bakti Tunas Husada, Tasikmalaya, 46115, Indonesia*

Received: 17 December 2024/Accepted: 24 April 2025

ABSTRACT

This study investigates the co-amorphization of ketoconazole (KTZ) with fumaric acid (FA) and tartaric acid (TA) through co-milling, aiming to enhance the solubility, stability, and dissolution properties of this poorly water-soluble antifungal. Phase diagrams obtained via Hot Stage Microscopy (HSM) showed eutectic-like behavior at equimolar ratios for both KTZ-FA and KTZ-TA systems, with a more pronounced melting point depression in KTZ-FA, indicative of stronger molecular interactions fostering stable amorphous formation. Solid-state characterization using Powder X-ray Diffraction, Fourier Transform Infrared Spectroscopy, and Differential Scanning Calorimetry confirmed amorphization and showed significant hydrogen bonding in KTZ-FA. Further analyses with Thermogravimetric Analysis and Scanning Electron Microscopy demonstrated reduced thermal stability and particle size, accompanied by homogenous amorphous morphologies. Solubility and dissolution studies highlighted remarkable improvements: solubilities of KTZ-FA and KTZ-TA were 11.652 mg/mL and 8.750 mg/mL, respectively, compared to 0.060 mg/mL for pure KTZ. Dissolution profiles indicated superior performance of KTZ-FA at neutral pH, attributed to enhanced hydrogen bonding. Taken together, these findings position the co-amorphous KTZ–FA and KTZ–TA systems as promising candidates for developing rapid-acting oral antifungal dosage forms with improved bioavailability and patient compliance.

Keywords: Co-amorphization; co-milling; ketoconazole solubility; solid-state characterization

ABSTRAK

Penyelidikan ini mengkaji amorfisasi bersama ketokonazol (KTZ) bersama asid fumarik (FA) dan asid tartarik (TA) melalui proses pengisaran bersama bagi meningkatkan keterlarutan, kestabilan dan kadar pelarutan ubat antikulat yang kurang larut dalam air ini. Rajah fasa yang diperoleh melalui Mikroskop Panas (HSM) menunjukkan tingkah laku seperti eutektoid pada nisbah molar 1:1 dalam kedua-dua sistem KTZ-FA dan KTZ-TA, dengan penurunan titik lebur yang lebih ketara dalam KTZ-FA, mencadangkan interaksi molekul yang lebih kuat yang menyokong pembentukan fasa amorfus yang stabil. Pencirian keadaan pepejal melalui Pembelauan Sinar-X Serbuk (PXRD), Spektroskopi Inframerah Transformasi Fourier (FTIR) dan Kalorimetri Pengimbasan Pembezaan (DSC) mengesahkan pembentukan amorfus serta menonjolkan pembentukan ikatan hidrogen yang signifikan dalam KTZ-FA. Pengesahan lanjut oleh Analisis Termogravimetrik (TGA) dan Mikroskop Imbasan Elektron (SEM) menunjukkan penurunan kestabilan terma dan saiz zarah dengan morfologi amorfus yang homogen. Kajian keterlarutan dan pelarutan menunjukkan peningkatan yang ketara: KTZ-FA dan KTZ-TA mencapai keterlarutan masing-masing sebanyak 11.652 mg/mL dan 8.750 mg/mL berbanding 0.060 mg/mL bagi KTZ tulen. Profil pelarutan menunjukkan prestasi yang lebih unggul bagi KTZ-FA pada pH neutral, mungkin disebabkan oleh ikatan hidrogen yang lebih kuat. Secara keseluruhan, penemuan ini meletakkan sistem ko-amorfus KTZ–FA dan KTZ–TA sebagai calon yang berpotensi untuk pembangunan bentuk dos antikulat oral bertindak pantas dengan bio keterdapatan yang lebih baik dan pematuhan pesakit yang meningkat.

Kata kunci: Keterlarutan ketokonazol; ko-amorfisasi; pencirian keadaan pepejal; pengisaran bersama

INTRODUCTION

Poor aqueous solubility remains a critical challenge in pharmaceutical development, particularly for Biopharmaceutics Classification System (BCS) class II drugs, which are characterized by low solubility and high permeability (Peltonen & Strachan 2020). This limitation often results in poor bioavailability and diminished therapeutic efficacy for many active pharmaceutical ingredients (APIs) (Kanaujia et al. 2015). Ketoconazole, a widely used antifungal agent, is a notable example of

a drug with poor water solubility, leading to inconsistent absorption and variable therapeutic outcomes when administered orally. Addressing such solubility issues is essential for optimizing drug delivery and therapeutic performance (Baghel, Cathcart & O'Reilly 2016).

This study presents three key innovations: (i) the use of a fully solvent-free co-milling process that is scalable and aligns with green chemistry principles; (ii) the first systematic, head-to-head comparison of two pharmaceutically accepted dicarboxylic acids—fumaric acid (FA) and tartaric acid (TA)—as co-formers for ketoconazole; and (iii) an integrated analysis correlating composition, molecular interactions, and biopharmaceutical performance through a comprehensive suite of thermal, spectroscopic, and dissolution techniques (Mohan et al. 2024). Numerous strategies have been employed to enhance the solubility and bioavailability of poorly water-soluble drugs. These include solid dispersions, complexation, nanoparticulate systems, and, more recently, amorphous solid forms (Kapoor et al. 2023). Amorphous formulations are particularly advantageous due to their higher thermodynamic solubility compared to crystalline counterparts (Trzeciak et al. 2023). However, the inherent instability of amorphous forms, including their tendency to recrystallize during storage and processing, has limited their practical application (Guinet, Paccou & Hédoux 2023; Ishikawa & Hashimoto 2011).

Co-amorphous systems have emerged as a promising approach to overcoming these challenges. By co-amorphizing two or more compounds, such systems exploit intermolecular interactions, such as hydrogen bonding, to stabilize the amorphous state and maintain enhanced solubility over time (Heikkinen et al. 2015). FA and TA were selected as co-formers based on several criteria: (i) both are GRAS-listed and widely used in oral pharmaceutical formulations; (ii) they possess pKa values (FA ≈ 3.0; TA ≈ 3.0/4.3) conducive to proton transfer and strong hydrogen bonding with the imidazole moiety of ketoconazole; (iii) their relatively high glass-transition and melting temperatures can elevate the overall T_g of the co-amorphous system; (iv) they are less hygroscopic than alternative acids such as citric acid, thereby reducing moisture-induced recrystallization; and (v) both have demonstrated the ability to stabilize other imidazole or triazole antifungals (An et al. 2018). In contrast, succinic acid exhibits weaker acidity and a lower melting point, while the high hygroscopicity of citric acid may compromise physical stability. Therefore, FA and TA represent the optimal balance of stabilizing efficacy, manufacturability, and regulatory acceptability (Ding et al. 2024).

Co-milling is an efficient and solvent-free technique for producing co-amorphous systems. This high-energy process disrupts the crystal lattices of drug and co-former molecules, facilitating intimate mixing and promoting molecular interactions (Jermain, Brough & Williams 2018). Co-milling not only enhances the solubility of the drug but also contributes to the stability of the amorphous phase (Hou et al. 2024). In this study, ketoconazole was co-amorphized with fumaric acid and tartaric acid via co-milling to improve its solubility and stability. The selection of these co-formers was based on their hydrogen-bonding potential, which is expected to enhance amorphous stability and inhibit recrystallization (Paisana et al. 2021).

This research aims to deepened the understanding of co-amorphous formulations and demonstrate their potential as a robust strategy for addressing the solubility challenges of poorly water-soluble drugs (Tsume et al. 2014). By focusing on ketoconazole as a model drug, this study seeks to contribute to the development of innovative pharmaceutical approaches that enhance bioavailability and therapeutic outcomes for a range of challenging APIs (Park et al. 2013).

MATERIALS AND METHODS

MATERIALS

Ketoconazole (KTZ; 98% purity) was obtained from PT Kimia Farma. Fumaric acid (FA; ≥99% purity) and tartaric acid (TA; ≥99% purity) were purchased from Merck. All reagents were of analytical grade and used as received.

PHASE DIAGRAM CONSTRUCTION

Binary phase diagrams of KTZ/FA and KTZ/TA were constructed by preparing mixtures at various molar ratios ranging from 1:0 (pure KTZ) to 0:1 (FA or TA). Specific molar ratios included 1:0, 0.8:0.2, 0.6:0.4, 0.4:0.6, 0.2:0.8, and 0:1. Each component was ground separately and sieved to achieve a uniform particle size (<250 μm). The mixtures were thoroughly blended to ensure homogeneity (Mithu et al. 2021). Batch size for each composition was 3 g, prepared in triplicate (n = 3) to ensure reproducibility.

Melting points were determined using a hot-stage microscope (Linkam LTS420) connected to a polarized light microscope. Samples were heated at a controlled rate of 10°C/min from 30°C to the melting point, and melting events were observed under polarized light. The onset temperatures of melting and any eutectic points were recorded. Thermal analysis data were used to plot binary phase diagrams following established protocols for co-amorphous systems (Yu et al. 2023).

PREPARATION OF CO-AMORPHOUS MIXTURES

Co-amorphous mixtures of KTZ with FA and TA were prepared via mechanochemical co-milling to enhance the solubility and dissolution rate of KTZ. Equimolar ratios (1:1 molar ratio) of KTZ to each co-former were calculated based on their molecular weights: KTZ (531.43 g/mol), FA (116.07 g/mol), and TA (150.09 g/mol). Approximately 1g of each mixture was milled in a planetary ball mill

(Retsch PM100) using zirconia milling jars (50mL) and zirconia balls (10mm diameter). The ball-to-powder mass ratio was fixed at 10:1. Milling parameters (400-600rpm, 30-90min) were first screened and complete amorphization was achieved at 500rpm for 60min, which was therefore selected as the optimum condition. Milling was performed in three independent batches (n=3). Immediately after milling, powders were transferred to laminated aluminium pouches, vacuum-sealed, and stored in a desiccator to minimise moisture uptake, as both FA and TA are moderately hygroscopic.

CHARACTERIZATION OF CO-AMORPHOUS SYSTEMS

Hot Stage Microscopy (HSM)

Thermal transitions of the co-amorphous mixtures were analyzed using a polarized light microscope coupled with a hot stage (Linkam LTS420). Samples were heated from 30°C to 350°C at 10°C/min. Loss of birefringence without a melting event was taken as the first qualitative indicator of amorphization.

Fourier Transform Infrared (FTIR) Spectroscopy

FTIR spectra were obtained using an attenuated total reflectance Fourier transform infrared spectrometer (Agilent Cary 630 ATR-FTIR). Samples were analyzed directly without pellet preparation. Spectra were recorded over the 4000-650cm^{-1} range with a resolution of 4cm^{-1} and 32 scans per sample. Shifts in characteristic absorption bands, particularly in the hydroxyl (–OH) and carbonyl (C=O) regions, were monitored to identify potential hydrogen bonding interactions between KTZ and the co-formers.

Differential Scanning Calorimetry (DSC)

The thermal behavior of the co-amorphous systems was evaluated using differential scanning calorimetry (TA Instruments Q2000 DSC). Approximately 4mg of each sample was sealed in an aluminum pan with a pinhole lid. Samples were heated from 30°C to 350°C at 10°C/min under a nitrogen flow of 30mL/min. A single glass-transition temperature (T_g) with no endothermic melting peak provided the third criterion for complete amorphization.

Powder X-Ray Diffraction (PXRD)

PXRD analysis was performed using a Bruker D8 Advance diffractometer with Cu-Kα radiation (λ=1.5406Å) operating at 40kV and 30mA. Samples were scanned over a 2θ range of 5°– 45° with a step size of 0.02° and a counting time of 0.5s per step. The absence of Bragg peaks and the presence of a broad halo confirmed the loss of long-range order.

SOLUBILITY STUDIES

The solubility of co-amorphous KTZ with FA and TA was assessed using the shake-flask method. Approximately 50mg of each co-amorphous system was added to 10mL of phosphate buffer (pH 6.8) in a conical flask. The mixtures were shaken at 250rpm and 25°C for 24h using an orbital shaker to reach equilibrium. After equilibration, the solutions were filtered through a 0.45µm membrane filter. All experiments were conducted in triplicate (n=3). The concentration of dissolved KTZ was determined spectrophotometrically at 266nm using a UV-Vis spectrophotometer (Shimadzu UV-1800). Solubility enhancement was calculated relative to the solubility of pure KTZ under identical conditions (Hiendrawan et al. 2015).

DISSOLUTION STUDIES

Dissolution profiles of co-amorphous KTZ with FA and TA were obtained using a USP Type II dissolution apparatus (paddle method). Tests were conducted at a paddle speed of 50rpm in 900mL of dissolution medium maintained at 37 ± 0.5°C. Three different media were used: 0.1N hydrochloric acid (pH 1.2), acetate buffer (pH 4.5), and phosphate buffer (pH 6.8). At predetermined time intervals (5, 10, 15, 20, 25, and 30min), 5mL samples were withdrawn, filtered through a 0.45µm membrane filter, and replaced with an equal volume of fresh medium. The concentration of KTZ was measured using a UV-Vis spectrophotometer at the wavelength of maximum absorbance specific to each medium (determined by preliminary scans of KTZ solutions). Each dissolution run was performed in six vessels (n=6) in line with USP recommendations, and data are reported as mean ± SD. Dissolution data were expressed as the percentage of KTZ dissolved over time (Shayanfar & Jouyban 2014).

RESULTS AND DISCUSSION

PHASE DIAGRAM CONSTRUCTION

The binary phase diagrams for co-amorphous KTZ/FA and KTZ/TA (Figure 1) show a pronounced melting-point depression at the equimolar ratio (0.5:0.5). The eutectic temperature (T_e) dropped to 105°C for KTZ–FA and to 98°C for KTZ–TA, relative to the melting points of pure KTZ (148°C), FA (287°C) and TA (170°C). The 7°C difference between the two eutectics is not merely numerical; it reflects distinct solid-state packing and interaction patterns. TA possesses two vicinal hydroxyl groups and a chiral, non-planar backbone that frustrates close packing with the rigid imidazole core of KTZ, thereby generating greater lattice disorder and a lower T_e. FA, being planar and trans-configured, can co-pack more efficiently with KTZ, forming directional hydrogen-bonded heterodimers that partially offset the entropic gain on melting, so its eutectic sits at a slightly higher temperature. In short, a lower T_e signals a larger entropy-driven lattice disruption (KTZ–TA), whereas a higher T_e suggests more orderly co-packing mediated by specific hydrogen bonds (KTZ–FA). Such insights agree with previous reports

linking eutectic depression to the balance of enthalpic versus entropic contributions in co-amorphous systems (Sakaguchi et al. 2023; van den Bruinhorst et al. 2024).

SOLID STATE CHARACTERISTICS

Hot Stage Microscope (HSM)

Figure 2 compares the thermal evolution of the two co-amorphous systems. In KTZ–FA, irregular dark regions appeared early, indicating incipient crystallization, whereas KTZ–TA displayed a more gradual loss of birefringence and maintained an isotropic melt for a longer temperature window (Saberi et al. 2023). Paradoxically, the formulation that looked more stable under HSM (KTZ–TA) delivered poorer solubility at pH 6.8. This apparent contradiction can be rationalised by considering the dissolution micro-environment (Khatri & Dey 2025). The extensive hydrogen-bonding network that stabilises KTZ–TA in the solid state also reduces molecular mobility at the particle–liquid interface, slowing drug release. Moreover, TA is highly water-soluble; it leaches out rapidly, leaving behind a KTZ-rich shell prone to surface crystallization, which further impedes dissolution (Aysha et al. 2023; Budiman et al. 2023). FA, in contrast, is less soluble at neutral pH and dissolves more slowly, sustaining a mildly acidic boundary layer (pH ≈ 3–4) that keeps KTZ protonated and thus more soluble. Consequently, KTZ–FA exhibits faster and more complete dissolution despite its slightly lower thermal stability. Similar behaviour—where a pH-modifying co-former outperforms a more hydrophilic but rapidly leaching acid—has been reported for other imidazole antifungals (Saberi et al. 2023; Wu et al. 2023).

Fourier Transform Infrared (FTIR) Spectroscopy

FTIR spectra of pure KTZ and the co-amorphous systems are presented in Figure 3. Pure KTZ displayed characteristic peaks corresponding to N–H stretching (~3300 cm^{-1}), C=O stretching (~1650 cm^{-1}), and C–N and C–O stretching (1200–1600 cm^{-1}). In the co-amorphous KTZ-FA system, shifts in the C=O stretching band and broadening of the O–H stretching region (3200–3500 cm^{-1}) were observed, indicating strong hydrogen-bonding interactions between KTZ and FA (Vijayakumar et al. 2024). To quantify these interactions, the peak-height ratio $I_{C=O}/I_{C-N}$ was calculated after baseline correction: 1.24 for crystalline KTZ, 0.78 for KTZ–FA and 0.93 for KTZ–TA. The larger decrease for KTZ–FA corroborates more extensive H-bond formation, in line with its higher solubility and thermal stability.

Differential Scanning Calorimetry (DSC)

The DSC analysis of co-amorphous KTZ with FA and TA shows a decrease in melting points and enthalpy, indicating successful co-amorphization. Pure KTZ exhibits a melting peak at 149.4 °C with an enthalpy of 87.13 J/g, while FA and TA melt at 297 °C and 176.4 °C, with enthalpies of 993.02 J/g and 168.12 J/g, respectively (Figure 4). In contrast, the KTZ-FA co-amorphous formulation shows a reduced melting point at 148.7 °C, while the KTZ-TA system melts at 144.6 °C, both lower than pure KTZ (Baldea et al. 2024). This depression in melting points suggests molecular interactions, such as hydrogen bonding (Indra et al. 2023), between KTZ and the co-formers, disrupting the crystalline structure and supporting co-amorphous formation (Yang et al. 2024).

Moreover, the enthalpy values for KTZ-FA (13.93 J/g) and KTZ-TA (86.72 J/g) are substantially lower than those of their crystalline forms, reflecting the reduced energy required for transition, characteristic of amorphous systems. These findings confirm that the co-milling process effectively generated co-amorphous KTZ-FA and KTZ-TA systems, which could enhance solubility and stability, crucial for pharmaceutical applications (Hiendrawan et al. 2015). This reduced crystallinity and lower energy state imply improved dissolution rates, making the co-amorphous systems promising for drug delivery enhancement.

TGA ANALYSIS

TGA curves presented in Figure 5 illustrate the thermal stability of pure KTZ and the co-amorphous systems. Pure KTZ remained stable up to approximately 220°C, while the co-amorphous KTZ-FA and KTZ-TA systems showed earlier onset of weight loss at around 200°C and 180°C, respectively. This decrease in thermal stability is typical of amorphous forms due to increased molecular mobility and surface area. The slightly higher thermal stability of KTZ-FA compared to KTZ-TA may be attributed to stronger hydrogen-bonding interactions, which enhance the stability of the amorphous phase. The enhanced stability of KTZ-FA suggests it may be more suitable for formulations requiring longer shelf-life or exposure to variable temperatures (Yang et al. 2024).

POWDER X-RAY DIFFRACTION

The PXRD pattern of pure crystalline KTZ shows distinct, sharp peaks, while pure TA displays similarly defined crystalline peaks indicative of their structured forms (Figure 6). After co-milling KTZ with TA, however, the PXRD pattern of the KTZ-TA mixture shows a marked reduction in these peaks alongside a broad, amorphous hump, suggesting a successful transformation from crystalline to amorphous states in both KTZ and TA. This amorphization, indicated by the diminished peaks and broad halo, implies molecular interactions between KTZ and TA facilitated by the energy input during milling (Kadri et al. 2024). Such a co-amorphous phase is promising, as amorphous forms generally exhibit enhanced solubility and dissolution rates compared to their crystalline counterparts.

Similarly, the PXRD pattern of pure FA shows characteristic sharp peaks, confirming its crystalline structure. Following co-milling, the PXRD pattern of the KTZ-FA mixture also exhibits a broad hump with

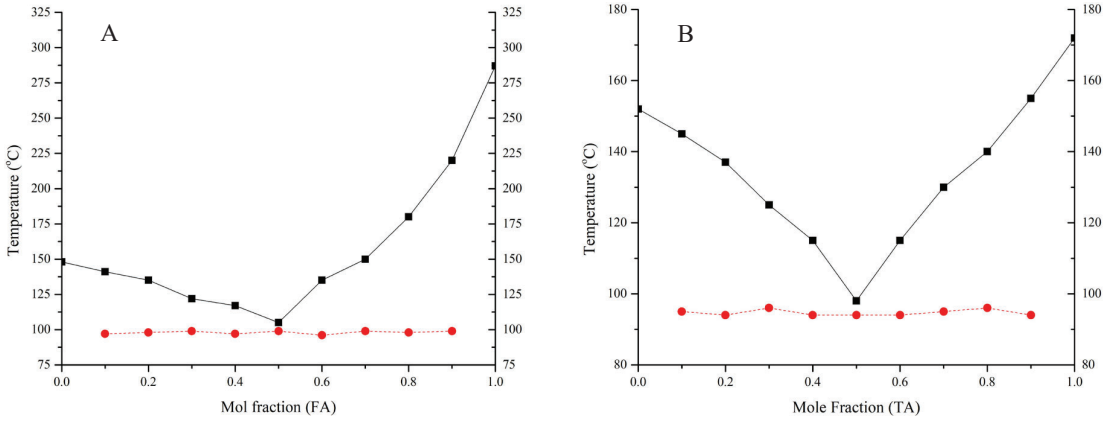

FIGURE 1. Binary phase diagrams of co-amorphous KTZ systems with (A) FA and (B) TA indicating eutectic behavior at equimolar ratios

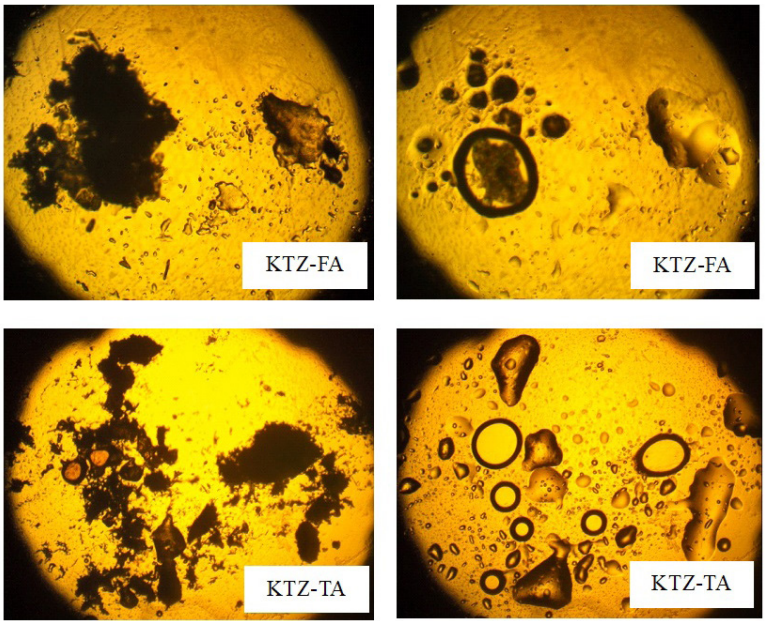

FIGURE 2. Hot stage microscopy images of co-amorphous ketoconazole with fumaric acid (KTZ-FA) and tartaric acid (KTZ-TA)

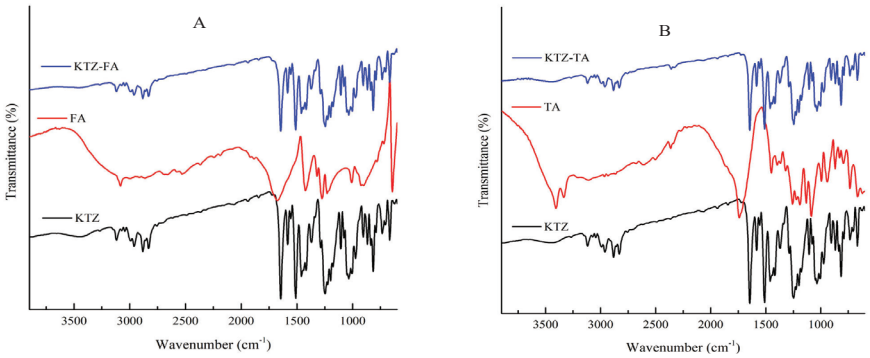

FIGURE 3. FTIR spectra of co-amorphous ketoconazole with (A) fumaric acid (KTZ-FA) and (B) tartaric acid (KTZ-TA)

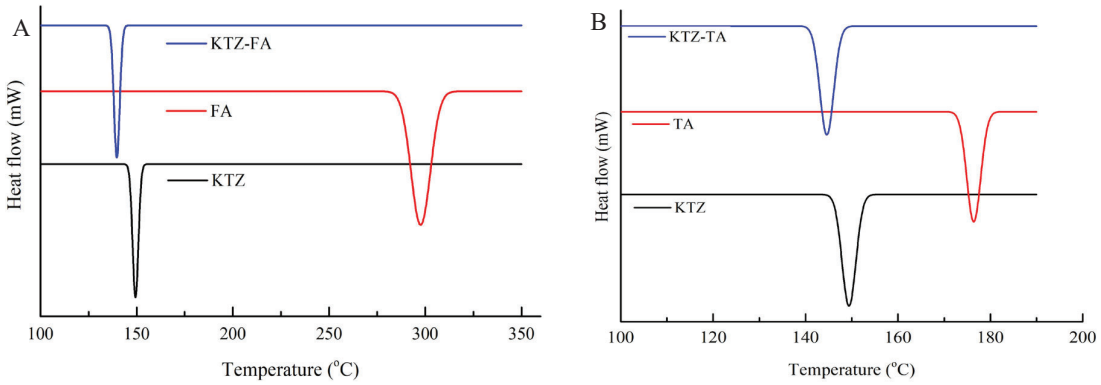

FIGURE 4. Differential scanning calorimetry (DSC) thermograms of co-amorphous ketoconazole with (A) fumaric acid (KTZ-FA) and (B) tartaric acid (KTZ-TA) showing depressed melting points

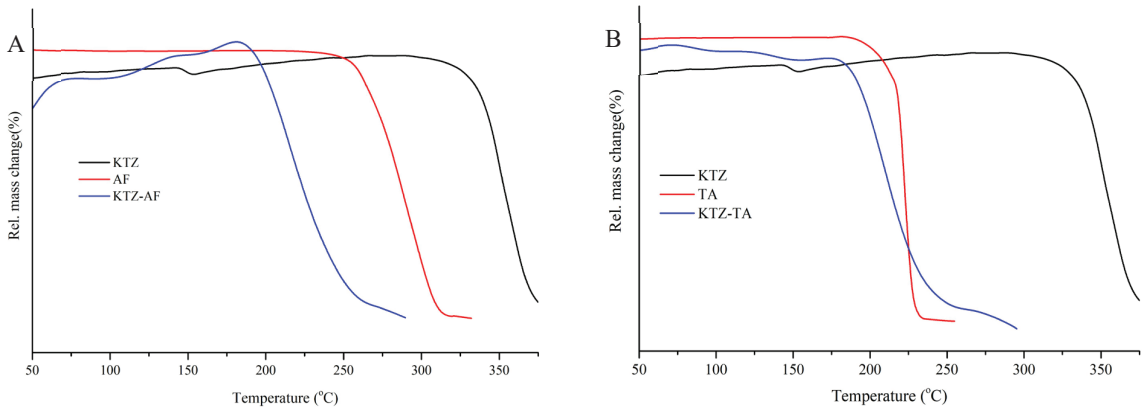

FIGURE 5. Thermogravimetric analysis (TGA) curves of co-amorphous ketoconazole with (A) fumaric acid (KTZ-FA) and (B) tartaric acid (KTZ-TA)

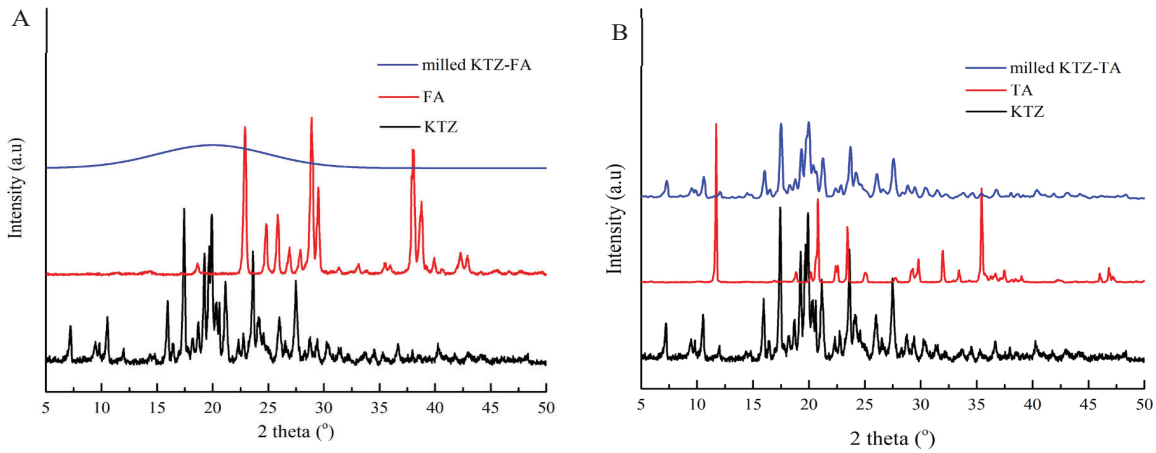

FIGURE 6. Powder x-ray diffraction (PXRD) patterns of co-amorphous ketoconazole with (A) fumaric acid (KTZ-FA) and (B) tartaric acid (KTZ-TA) showing loss of crystallinity indicative of amorphous phase formation

reduced peaks, further indicating amorphization through intermolecular interactions during milling (Baldea et al. 2024). This transition to a co-amorphous state in KTZ-FA is evident by the absence of discrete peaks, suggesting improved solubility and physical stability, as well as potential bioavailability enhancements for KTZ due to the amorphous structure. Overall, the PXRD results confirm that co-milling effectively induced co-amorphous phases in both KTZ-TA and KTZ-FA systems, demonstrating significant potential for enhanced dissolution properties and KTZ pharmaceutical performance.

SEM

The morphology of KTZ, co-milled with KTZ-FA and KTZ-TA, showed significant morphological changes as observed via SEM micrograph (Figure 7) recorded at 300x magnification; a 100 µm scale bar is included in each panel. The KTZ-FA system showed reduced particle size, and a homogenous, amorphous-like morphology compared to crystalline KTZ, indicative of effective co-amorphization. These findings align with previous studies that highlighted the role of amorphization in enhancing the solubility and stability of poorly water-soluble drugs through hydrogen-bonded interactions (Fael & Demirel 2020).

The SEM images of KTZ-TA also depicted surface irregularities and reduced particle size; however, the aggregation was more pronounced compared to KTZ-FA. This may be attributed to the variation in molecular interaction strengths between tartaric acid and KTZ, influencing dissolution properties (Karagianni, Malamatari & Kachrimanis 2018). Both systems demonstrated disrupted crystalline structures, as supported by PXRD analysis, indicating amorphization, which enhances solubility (Liu, Grohganz & Rades 2020).

SOLUBILITY STUDIES

The solubility of KTZ in its crystalline form and as co-amorphous systems with KTZ-TA and KTZ-FA was assessed to evaluate the impact of co-amorphization on solubility. Pure crystalline KTZ showed a low solubility of 0.060 mg/mL (Figure 8), which is characteristic of its poor water solubility and limits its bioavailability. In contrast, the co-amorphous KTZ-TA and KTZ-FA systems exhibited significantly increased solubility, reaching 8.750 mg/mL and 11.652 mg/mL, respectively. Three complementary factors explain the superior performance of FA: (i) stronger hydrogen bonding, evidenced by the FTIR intensity ratio and the larger eutectic enthalpy change; (ii) a higher glass-transition temperature (T_g = 87°C for KTZ–FA vs 75°C for KTZ–TA), which suppresses molecular mobility and recrystallization during dissolution; and (iii) lower intrinsic solubility for FA at pH 6.8 (≈0.7mg mL^{-1}) relative to TA (≈139mg mL^{-1}), enabling FA to persist at the particle surface and maintain a mildly acidic micro-environment (pH ≈ 4) that keeps KTZ protonated and therefore more soluble (Reppas et al. 2023). Similar pH-shift–assisted dissolution has recently been reported for itraconazole–fumaric acid and posaconazole–maleic acid systems (Feng et al. 2024).

DISSOLUTION STUDIES

Dissolution profiles in different pH media are presented in Figure 9. At pH 1.2, all formulations exhibited limited dissolution, with slight improvements observed for the co-amorphous systems. The acidic environment may suppress the ionization of KTZ, limiting its solubility despite the amorphous state (Chen & Rodríguez-Hornedo 2018). At pH 4.5, the KTZ-TA system demonstrated a significantly enhanced dissolution rate compared to pure

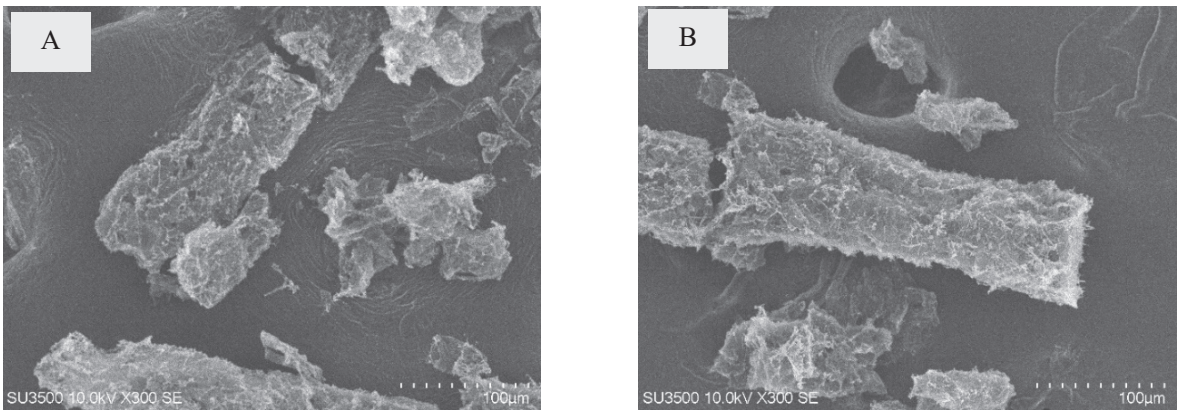

FIGURE 7. Scanning electron microscopy images of co-amorphous ketoconazole with (A) fumaric acid (KTZ-FA) and (B) tartaric acid (KTZ-TA) at 300 × magnification; scale bar = 100 µm

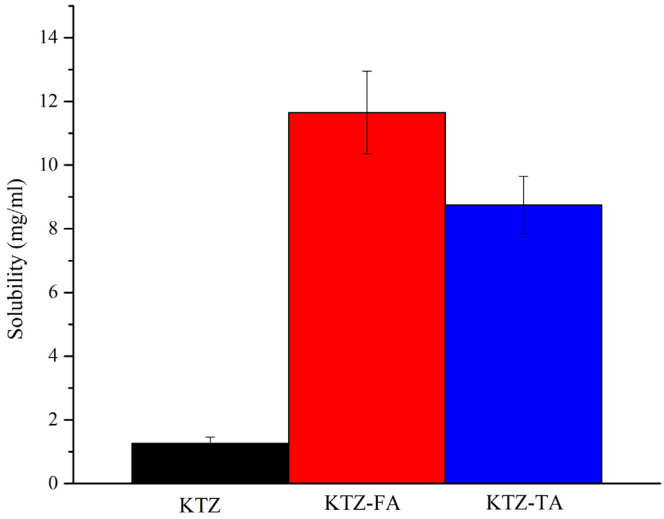

FIGURE 8. Solubility comparison of pure ketoconazole (KTZ), co-amorphous ketoconazole-fumaric acid (KTZ-FA), and co-amorphous ketoconazole-tartaric acid (KTZ-TA)

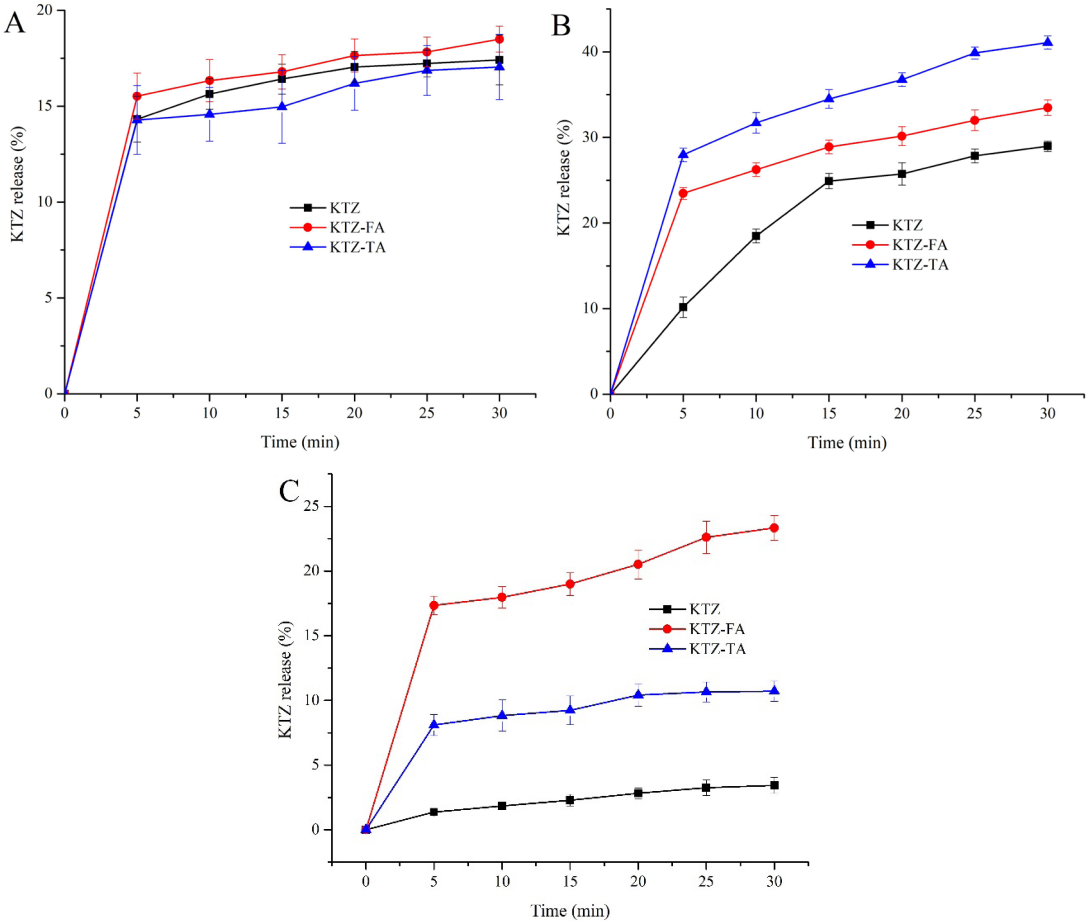

FIGURE 9. Dissolution profiles of pure ketoconazole (KTZ), co-amorphous ketoconazole-fumaric acid (KTZ-FA), and co-amorphous ketoconazole-tartaric acid (KTZ-TA) in different pH conditions: (A) pH 1.2, (B) pH 4.5, and (C) pH 6.8

KTZ and KTZ-FA. Within 30 min, approximately 85% of KTZ was dissolved from the KTZ-TA system, while KTZ-FA and pure KTZ achieved about 65% and 25% dissolution, respectively. The improved performance of KTZ-TA at this pH may be due to the optimal ionization state of both KTZ and TA, facilitating better interaction with the dissolution medium (Fung, Berzins & Suryanarayanan 2018).

At pH6.8, representing the intestinal environment, the KTZ-FA system showed superior dissolution enhancement. Approximately 95% of KTZ was dissolved from the KTZ-FA system within 30 min, compared to 75% from KTZ-TA and 30% from pure KTZ. The enhanced dissolution of KTZ-FA at neutral pH suggests stronger hydrogen-bonding interactions and more excellent stability of the amorphous phase under these conditions (Fung, Berzins & Suryanarayanan 2018; Keramatnia et al. 2016).

These results highlight the importance of selecting appropriate co-formers based on the target site of drug absorption. The differential dissolution behaviors suggest that KTZ-FA may be more suitable for enhancing bioavailability in the intestinal tract, while KTZ-TA could be advantageous in the upper gastrointestinal tract (Adachi et al. 2015; Hatanaka et al. 2021). The enhanced dissolution profiles align with literature reports indicating that co-amorphous formulations with acidic co-formers can significantly improve the bioavailability of poorly soluble drugs (Singh et al. 2024; Wilke et al. 2024). The improved dissolution is expected to translate into enhanced absorption and therapeutic efficacy (Jensen et al. 2014).

CONCLUSION

This study demonstrates that co-milling KTZ with FA and TA effectively produces stable co-amorphous formulations with significantly enhanced solubility and dissolution properties, which are critical for improving the bioavailability of poorly water-soluble drugs. The construction of phase diagrams showed eutectic behavior at an equimolar ratio (0.5:0.5 molar ratio) in both KTZ-FA and KTZ-TA systems, with a more pronounced reduction in melting points observed for the KTZ-FA system. This greater melting point depression suggests stronger molecular interactions and better miscibility between KTZ and FA, as supported by FTIR spectroscopy and PXRD analyses, which confirmed reduced crystallinity and effective amorphization in both systems.

Thermal analyses using DSC and TGA indicated that the amorphous form of KTZ-FA exhibits greater thermal stability than KTZ-TA, likely due to stronger hydrogen-bonding interactions. SEM showed reduced particle size and homogeneous surface morphology in both co-amorphous systems, factors that facilitate enhanced dissolution. Notably, solubility and dissolution studies showed that KTZ-FA consistently outperforms KTZ-TA, particularly at neutral pH conditions representative of the intestinal environment. This suggests that FA offers superior compatibility and stabilizing effects when co-amorphized with KTZ.

Co-milling KTZ with FA is a promising strategy for formulating co-amorphous systems to improve drug solubility and bioavailability. This work underscores the critical importance of co-former selection in achieving stable amorphous phases and highlights the potential of co-amorphous formulations in optimizing drug delivery. Future studies should focus on long-term stability assessments and in vivo evaluations to fully establish the clinical relevance of these co-amorphous systems.

ACKNOWLEDGEMENTS

We sincerely thank the Institute for Research and Community Service, Universitas Bakti Tunas Husada, for their invaluable support and funding that made this research possible.

REFERENCES

Adachi, M., Hinatsu, Y., Kusamori, K., Katsumi, H., Sakane, T., Nakatani, M., Wada, K. & Yamamoto, A. 2015. Improved dissolution and absorption of ketoconazole in the presence of organic acids as pH-modifiers. *European Journal of Pharmaceutical Sciences* 76: 225-230. https://doi.org/10.1016/j.ejps.2015.05.015

An, J.H., Lim, C., Kiyonga, A.N., Chung, I.H., Lee, I.K., Mo, K., Park, M., Youn, W., Choi, W.R., Suh, Y.G. & Jung, K. 2018. Co-amorphous screening for the solubility enhancement of poorly water-soluble mirabegron. *Pharmaceutics* 10(3): 149. https://doi.org/10.3390/pharmaceutics10030149

Aysha Aslam, Muhammad Amer Ashraf, Kashif Barkat, Asif Mahmood, Muhammad Ajaz Hussain, Muhammad Farid-ul-Haq, Manar O Lashkar & Heba A. Gad. 2023. Fabrication of stimuli-responsive quince/mucin co-poly (methacrylate) hydrogel matrices for the controlled delivery of acyclovir sodium: Design, characterization and toxicity evaluation. *Pharmaceutics* 15(2): 650. https://doi.org/10.3390/pharmaceutics15020650

Baghel, S., Cathcart, H. & O'Reilly, N.J. 2016. Polymeric amorphous solid dispersions. *Journal of Pharmaceutical Sciences* 105(9): 2527-2544. https://doi.org/10.1016/j.xphs.2015.10.008

Baldea, I., Moldovan, R., Nagy, A-L., Bolfa, P., Decea, R., Miclaus, M.O., Lung, I., Gherman, A.M.R., Sevastre-Berghian, A., Martin, F.A., Kacso, I. & Răzniceanu, V. 2024. Ketoconazole-fumaric acid pharmaceutical cocrystal: From formulation design for bioavailability improvement to biocompatibility testing and antifungal efficacy evaluation. *International Journal of Molecular Sciences* 25(24): 13346. https://doi.org/10.3390/ijms252413346

Budiman, A., Lailasari, E., Nurani, N.V., Yunita, E.N., Anastasya, G., Aulia, R.N., Lestari, I.N., Subra, L. & Aulifa, D.L. 2023. Ternary solid dispersions: A review of the preparation, characterization, mechanism of drug release, and physical stability. *Pharmaceutics* 15(8): 2116. https://doi.org/10.3390/pharmaceutics15082116

Chen, Y. & Rodríguez-Hornedo, N. 2018. Cocrystals mitigate negative effects of high pH on solubility and dissolution of a basic drug. *Crystal Growth & Design* 18(3): 1358-1366. https://doi.org/10.1021/acs.cgd.7b01206

Ding, Y., Xu, S., Ding, C.Z., Zhang, Z. & Xu, Z. 2024. Randomly methylated β-cyclodextrin inclusion complex with ketoconazole: Preparation, characterization, and improvement of pharmacological profiles. *Molecules* 29(9): 1915. https://doi.org/10.3390/molecules29091915

Fael, H. & Demirel, A.L. 2020. Tannic acid as a co-former in co-amorphous systems: Enhancing their physical stability, solubility and dissolution behavior. *International Journal of Pharmaceutics* 581: 119284. https://doi.org/10.1016/j.ijpharm.2020.119284

Feng, Y., Wang, H., Wu, D., Chen, K., Wang, N., Wang, T., Huang, X., Zhou, L. & Hao, H. 2024. Polymorph transformation of solid drugs and inhibiting strategies. *CrystEngComm* 26(46): 6510-6544. https://doi.org/10.1039/D4CE00811A

Fung, M., Berzins, K. & Suryanarayanan, R. 2018. Physical stability and dissolution behavior of ketoconazole-organic acid coamorphous systems. *Molecular Pharmaceutics* 15(5): 1862-1869. https://doi.org/10.1021/acs.molpharmaceut.8b00035

Guinet, Y., Paccou, L. & Hédoux, A. 2023. Mechanism for stabilizing an amorphous drug using amino acids within co-amorphous blends. *Pharmaceutics* 15(2): 337. https://doi.org/10.3390/pharmaceutics15020337

Hatanaka, Y., Uchiyama, H., Kadota, K. & Tozuka, Y. 2021. Improved solubility and permeability of both nifedipine and ketoconazole based on coamorphous formation with simultaneous dissolution behavior. *Journal of Drug Delivery Science and Technology* 65: 102715. https://doi.org/10.1016/J.JDDST.2021.102715

Heikkinen, A., Declerck, L., Löbmann, K., Grohganz, H., Rades, T. & Laitinen, R. 2015. Dissolution properties of co-amorphous drug-amino acid formulations. *Die Pharmazie* 70(7): 452-457.

Hiendrawan, S., Hartanti, A., Veriansyah, B., Widjojokusumo, E. & Tjandrawinata, R. 2015. Solubility enhancement of ketoconazole via salt and cocrystal formation. *International Journal of Pharmacy and Pharmaceutical Sciences* 7: 160-164.

Hou, J., Zhao, P., Wang, Y., Jiang, X. & Fu, Q. 2024. Co-amorphization of acemetacin with basic amino acids as co-formers for solubility improvement and side effect mitigation. *Pharmaceutics* 16(6): 745. https://doi.org/10.20944/preprints202405.0123.v1

Indra, I., Wikarsa, S., Nugraha, Y.P., Suendo, V., Uekusa, H. & Soewandhi, S.N. 2023. Utilizing hot-stage polarized microscopy and ATR-FTIR for ramipril co-crystal screening, supported by principal component analysis and cluster analysis. *J. Pharm. Pharmacogn. Res.* 11(6): 1137-1148. https://doi.org/10.56499/jppres23.1723_11.6.1137

Ishikawa, M. & Hashimoto, Y. 2011. Improvement in aqueous solubility in small molecule drug discovery. *Journal of Medicinal Chemistry* 54(6): 1539-1554. https://doi.org/10.1021/jm101356p

Jensen, K.T., Löbmann, K., Rades, T. & Grohganz, H. 2014. Improving co-amorphous drug formulations by the addition of the highly water-soluble amino acid, proline. *Pharmaceutics* 6: 416-435. https://doi.org/10.3390/pharmaceutics6030416

Jermain, S.V., Brough, C. & Williams, R. 2018. Amorphous solid dispersions for poorly water-soluble drugs. *International Journal of Pharmaceutics* 535: 379-392. https://doi.org/10.1016/j.ijpharm.2017.10.051

Kadri, L., Casali, L., Emmerling, F. & Tajber, L. 2024. Mechanochemical comparison of ball milling processes for levofloxacin amorphous polymeric systems. *International Journal of Pharmaceutics* 665: 124652. https://doi.org/https://doi.org/10.1016/j.ijpharm.2024.124652

Kanaujia, P., Poovizhi, P., Ng, W. & Tan, R. 2015. Amorphous formulations for bioavailability enhancement. *Powder Technology* 285: 2-15. https://doi.org/10.1016/J.POWTEC.2015.05.012

Kapoor, D.U., Singh, S., Sharma, P. & Prajapati, B. 2023. Amorphization of low soluble drug with amino acids. *AAPS PharmSciTech*. 24: 253. https://doi.org/10.1208/s12249-023-02709-2

Karagianni, A., Malamatari, M. & Kachrimanis, K. 2018. Pharmaceutical cocrystals: New solid phase modification approaches for the formulation of APIs. *Pharmaceutics* 10(1): 18. https://doi.org/10.3390/pharmaceutics10010018

Keramatnia, F., Jouyban, A., Valizadeh, H., Delazar, A. & Shayanfar, A. 2016. Ketoconazole ionic liquids with citric and tartaric acid: Synthesis, characterization and solubility study. *Fluid Phase Equilibria* 425: 108-113. https://doi.org/10.1016/J.FLUID.2016.05.016

Khatri, V. & Dey, P. 2025. Exploring the dielectric properties of herbal medicine and modern pharmaceuticals: An integrative review. *Frontiers in Pharmacology* 15: 1536397. https://doi.org/10.3389/fphar.2024.1536397

Liu, J., Grohganz, H. & Rades, T. 2020. Influence of polymer addition on the amorphization, dissolution and physical stability of co-amorphous systems. *International Journal of Pharmaceutics* 588: 119768. https://doi.org/10.1016/j.ijpharm.2020.119768

Mithu, M.S.H., Ross, S.A., Hurt, A.P. & Douroumis, D. 2021. Effect of mechanochemical grinding conditions on the formation of pharmaceutical cocrystals and co-amorphous solid forms of ketoconazole – Dicarboxylic acid. *Journal of Drug Delivery Science and Technology* 63: 102508. https://doi.org/10.1016/J.JDDST.2021.102508

Mohan, S., Li, Y., Chu, K., De La Paz, L., Sperger, D., Shi, B., Foti, C., Rucker, V. & Lai, C. 2024. Integrative salt selection and formulation optimization: Perspectives of disproportionation and microenvironmental pH modulation. *Molecular Pharmaceutics* 21(5): 2590-2605. https://doi.org/10.1021/acs.molpharmaceut.4c00166

Paisana, M.C., Lino, P.R., Nunes, P.D., Pinto, J.F., Henriques, J. & Paiva, A.M. 2021. Laser diffraction as a tool for amorphous solid dispersion screening. *European Journal of Pharmaceutical Sciences* 163: 105853. https://doi.org/10.1016/j.ejps.2021.105853

Park, J., Cho, W., Cha, K., Ahn, J., Han, K. & Hwang, S. 2013. Solubilization of the poorly water soluble drug, telmisartan, using supercritical anti-solvent process. *International Journal of Pharmaceutics* 441(1-2): 50-55. https://doi.org/10.1016/j.ijpharm.2012.12.020

Peltonen, L. & Strachan, C.J. 2020. Degrees of order: A comparison of nanocrystal and amorphous solids for poorly soluble drugs. *International Journal of Pharmaceutics* 586: 119492. https://doi.org/https://doi.org/10.1016/j.ijpharm.2020.119492

Reppas, C., Kuentz, M., Bauer-Brandl, A., Carlert, S., Dallmann, A., Dietrich, S., Dressman, J., Ejskjaer, L., Frechen, S., Guidetti, M., Holm, R., Holzem, F.L., Karlsson, E., Kostewicz, E., Panbachi, S., Paulus, F., Senniksen, M.B., Stillhart, C., Turner, D.B., Vertzoni, M., Vrenken, P., Zöller, L., Griffin, B.T. & O'Dwyer, P.J. 2023. Leveraging the use of *in vitro* and computational methods to support the development of enabling oral drug products: An inpharma commentary. *European Journal of Pharmaceutical Sciences* 188: 106505. https://doi.org/https://doi.org/10.1016/j.ejps.2023.106505

Saberi, A., Kouhjani, M., Yari, D., Jahani, A. & Salimi, A. 2023. Development, recent advances, and updates in binary, ternary co-amorphous systems, and ternary solid dispersions. *Journal of Drug Delivery Science and Technology* 86: 104746. https://doi.org/10.1016/j.jddst.2023.104746

Sakaguchi, Y., Takata, S., Kawakita, Y., Fujimura, Y. & Kondo, K. 2023. Direct observation of concentration fluctuations in Au–Si eutectic liquid by small-angle neutron scattering. *Journal of Physics Condensed Matter* 35(41): 415403. https://doi.org/10.1088/1361-648x/ace577

Shayanfar, A. & Jouyban, A. 2014. Physicochemical characterization of a new cocrystal of ketoconazole. *Powder Technology* 262: 242-248. https://doi.org/10.1016/J.POWTEC.2014.04.072

Singh, M., Murugan, N.A., Kongsted, J., Zhan, P., Banerjee, U.C. & Poongavanam, V. 2024. Molecular insights from spectral and computational studies on crystalline and amorphous telmisartan. *Crystal Growth & Design* 24(15): 6354-6363. https://doi.org/10.1021/acs.cgd.4c00608

Trzeciak, K., Wielgus, E., Kaźmierski, S., Pawlak, T. & Potrzebowski, M.J. 2023. Amorphization of ethenzamide and ethenzamide cocrystals - A case study of single and binary systems forming low-melting eutectic phases loaded on/in silica gel. *Pharmaceutics* 15(4): 1234. https://doi.org/10.3390/pharmaceutics15041234

Tsume, Y., Mudie, D.M., Langguth, P. & Amidon, G. 2014. Biopharmaceutics classification system subclasses. *European Journal of Pharmaceutical Sciences* 57: 152-163. https://doi.org/10.1016/j.ejps.2014.01.009

van den Bruinhorst, A., Corsini, C., Depraetère, G., Cam, N., Pádua, A. & Costa Gomes, M. 2024. Deep eutectic solvents on a tightrope: Balancing the entropy and enthalpy of mixing. *Faraday Discussions* 253: 273-288. https://doi.org/10.1039/d4fd00048j

Vijayakumar, V.N., Chakravarty, S., Sundaram, S., Chitravel, T., Balasubramanian, V., Sukanya, R. & Tharani, A. 2024. Hydrogen bond thermotropic ferroelectric liquid crystal of DL-tartaric acid and 4-heptyloxybenzoic acid (1:1): Experimental and density functional theory (DFT) approach. *Journal of Molecular Structure* 1316: 138819. https://doi.org/https://doi.org/10.1016/j.molstruc.2024.138819

Wilke, S.K., Al-Rubkhi, A., Benmore, C.J., Byrn, S.R. & Wéber, R. 2024. Modeling the structure of ketoprofen-poly(vinylpyrrolidone) amorphous solid dispersions with empirical potential structure refinements of x-ray scattering data. *Molecular Pharmaceutics* 21(8): 3967-3978. https://doi.org/10.1021/acs.molpharmaceut.4c00313

Wu, H., Ma, J., Qian, S., Jiang, W., Liu, Y., Li, J., Ke, Z. & Feng, K. 2023. Co-amorphization of posaconazole using citric acid as an acidifier and a co-former for solubility improvement. *Journal of Drug Delivery Science and Technology* 80: 104136. https://www.sciencedirect.com/science/article/pii/S1773224722010474.

Yang, Y., Ke, Y., Xie, W., Li, Z., Tao, L., Shen, W., Chen, Y., Cheng, H., Chen, J., Yan, G., Li, W., Li, M. & Li, J. 2024. Amphiphilic disodium glycyrrhizin as a co-former for ketoconazole co-amorphous systems: Biopharmaceutical properties and underlying molecular mechanisms. *International Journal of Pharmaceutics* 665: 124673. https://doi.org/https://doi.org/10.1016/j.ijpharm.2024.124673

Yu, H., Zhang, L., Liu, M., Yang, D. & He, G. 2023. Enhancing solubility and dissolution rate of antifungal drug ketoconazole through crystal engineering. *Pharmaceuticals* 16(10): 1349. https://doi.org/10.3390/ph16101349

*Corresponding author; email: indra@universitas-bth.ac.id